AIAA JOURNAL
Vol. 40, No. 9, September 2002

Modeling of Tapered Sandwich Panels Using a High-Order Sandwich Theory Formulation

Ole Thybo Thomsen*
Aalborg University, DK-9220 Aalborg East, Denmark
and
Jack R. Vinson†
University of Delaware, Newark, Delaware 19716

A newly developed high-order sandwich theory formulation is presented, which enables the analysis of sandwich beams or plates with variable core thickness. The faces are assumed to be of constant thickness and may be inclined arbitrary angles α_1 and α_2, respectively, relative to the sandwich panel reference plane. The core thickness may change linearly over the length of the sandwich panel. The core is modeled as a specially orthotropic solid possessing stiffness in the out-of-plane direction only, thus including the transverse core flexibility in the modeling. The faces are modeled as laminated beams or plates including bending–stretching coupling and transverse shear effects. To validate the proposed high-order theory, the numerical results are compared with results obtained from finite element analysis, and a close match is observed. Furthermore, to demonstrate the features of the developed high-order sandwich theory formulation, numerical results obtained for two different types of tapered sandwich beams in three-point bending are presented. The characteristics of the elastic responses of the two sandwich panel configurations are compared with special emphasis on the complicated interaction between the faces through the core material. The analyses show that severe localized bending effects are displayed in the vicinity of load introduction and support points and in the vicinity of points/locations of abrupt geometric changes. These localized bending effects induce severe stress concentrations and may severely endanger the structural integrity of the sandwich panels under consideration.

Nomenclature

A^i_{11}	=	extensional stiffness of faces, N · mm^{-1}
B^i_{11}	=	coupling stiffness of faces, N
C^i_{55}	=	transverse shear stiffness of faces, N · mm^{-1}
c	=	core thickness, mm
c_i	=	partial core thickness in tapered sandwich panel, $c_1 + c_2$, mm
c_i^0, c_i^{end}	=	initial and end values of partial core thicknesses in tapered sandwich panel, mm
c_k	=	initial and final values of core thickness c over length L, where $k = 0, e$, mm
D^i_{11}	=	bending stiffness of faces, N · mm
E_c	=	Young's modulus of core, N · mm^{-2}
E^i_{11}	=	Young's modulus of faces, N · mm^{-2}
f_i	=	thickness of faces, mm
G_c	=	shear modulus of core, N · mm^{-2}
G^i_{13}	=	transverse shear modulus of faces, N · mm^{-2}
L	=	length of tapered sandwich panel or half-length of sandwich beam in three-point bending, mm
L_j	=	partial lengths of combined section sandwich beam in three-point bending, where $j = a, b$, $L = L_a + L_b$, mm
M_i	=	bending moment resultant in faces, N
m_i, n_i, q_i	=	distributed moments, in-plane face load, and out-of-plane face loads, MPa
N_i	=	normal stress resultant in faces, N · mm^{-1}
Q_i	=	transverse shear stress resultant in faces, N · mm^{-1}
Q^i_{11}	=	in-plane stiffness coefficients for faces, N · mm^{-2}
Q^i_{55}	=	transverse shear stiffness coefficient for faces, N · mm^{-2}
u_c	=	in-plane (horizontal) displacement of core material, mm
u_i	=	in-plane displacement of faces in local face coordinates, mm
u_{0i}	=	in-plane displacement of midplanes of faces, mm
w_c	=	out-of-plane (vertical) displacement of core, mm
w_i	=	out-of-plane displacements of faces in local face coordinates, mm
x	=	horizontal (in-plane) coordinate, mm
x_c	=	horizontal (in-plane) core midplane coordinate, mm
z	=	vertical (out-of-plane) coordinate, mm
z_c	=	out-of-plane (vertical or horizontal) coordinate of core, mm
α_i	=	inclination angle of faces in tapered sandwich panel, rad
β_i	=	rotation of normals to face midplanes, rad
Γ_i	=	number of plies in face laminates
$\gamma_{\xi\zeta i}$	=	transverse shear strain in faces
δ_i	=	slopes of faces
ε_{0i}	=	normal strains in faces
θ	=	angular coordinate in curved sandwich panel, rad
κ_i	=	face curvatures, mm^{-1}
ν^i_{12}, ν^i_{21}	=	in-plane Poisson's ratios of faces
ξ_i, ζ_i	=	local face coordinates, mm
σ^j_f	=	core transverse normal stresses transformed into local face coordinates at top ($j = t$) and bottom ($j = b$) core/face boundaries, N · mm^{-2} (MPa)
σ_i^{outer}, σ_i^{inner}	=	stresses in outer and inner fibers of the faces, N · mm^{-2} (MPa)
σ_z	=	core transverse normal stress, N · mm^{-2} (MPa)
τ^j_f	=	core shear stresses transformed into local face coordinates at top, $j = t$, and bottom, $j = b$, core/face boundaries, N · mm^{-2}

Received 28 February 2001; revision received 15 February 2002; accepted for publication 14 March 2002.

*Head of Institute and Professor, Institute of Mechanical Engineering, Pontoppidanstræde 101; ott@ime.auc.dk. Member AIAA.

†Professor, Department of Mechanical Engineering, 126 Spencer Laboratory; vinson@me.udel.edu. Fellow AIAA.

τ_{xz} = core shear stress, $N \cdot mm^{-2}$ (MPa)
$\chi_j(x, z)$ = distribution functions for core displacements and stresses, where $j = 1, \ldots, 5$

Introduction

STRUCTURAL sandwich panels can be considered as a special type of composite laminate where two (or more) thin, stiff, strong and relatively dense faces (which may themselves be composite laminates) are separated by a thick, lightweight, and compliant core material. Such sandwich structures have gained widespread acceptance as an excellent way to obtain extremely lightweight components and structures with very high bending stiffness, high strength, and high buckling resistance.[1,2]

Symmetric sandwich panels with constant core and face thicknesses represent the simplest possible design configuration that will provide sufficiently lightweight structures for many purposes. However, if sandwich structures that are highly optimized with respect to weight are required, it is often necessary to use asymmetric sandwich panels with variable core and face thicknesses.

Sandwich structures are notoriously sensitive to failure by the application of concentrated loads, at points or lines of support, because of localized bending effects induced in the vicinity of points of geometric and material discontinuities. The reason for this is that, although sandwich structures are well suited for the transfer of overall bending and shearing loads, localized shearing and bending effects, as mentioned, induce severe through-thickness shear and normal stresses. These through-thickness stress components can be of significant magnitude and may in many cases approach or exceed the allowable stresses in the core material, in the faces as well as in the interfaces between the core and the faces.[1,3,4]

Sandwich panels with varying geometry are likely to experience localized bending and shearing effects (as discussed) to a larger extent than flat sandwich panels of constant geometry. Varying geometry in this context refers to sandwich panels with variable core and face thicknesses, as well as sandwich panels where a change of geometry occurs, for example, a transition from flat to tapered or similar.

Very little research has been done to investigate such geometrical change effects in sandwich panels. Exceptions from this are the works presented by Thomsen and Vinson,[5,6] and by Skvortsov et al.,[7] which include the analysis of transition zones between flat and curved sandwich panels. Furthermore, tapering effects in sandwich panels were treated also in Ref. 6, as well as by Kassapoglou.[8] The latter reference is concerned especially with so-called rampdowns, where sandwich panels are thinned down to monolithic laminates. Such rampdowns are made to provide for the mounting of mechanical fasteners or adhesive bonding.

The objective of the work presented was to develop a general formulation for the analysis of sandwich beams or plates with variable core thickness. The model is based on a high-order sandwich theory formulation, which includes the transverse flexibility of the core material. This enables the face sheets to deflect differently under the action of external loading, thus making it possible to quantify and evaluate the localized bending effects (as described), as well as the overall bending and shearing action effects.

Modeling

Figure 1 shows the principal geometric layout of the considered type of tapered sandwich panel section. For simplicity, the faces are assumed to be of constant thickness and may be inclined arbitrary angles α_1 and α_2, respectively, relative to the sandwich panel reference plane (defined by the Cartesian coordinate system x and z_c). Flat/straight sandwich panels can be analyzed by setting the inclination angles α_1 and α_2 to zero. The thickness of the core material may change linearly over the length of the sandwich panel. Because the structural response is likely to include significant core shear and transverse normal stresses, as described in the Introduction, the modeling is performed using a high-order formulation in which the elastic response of each face laminate is accounted for and in which the transverse core flexibility is included. Thus, the model allows the sandwich panel thickness to change during deformation, and

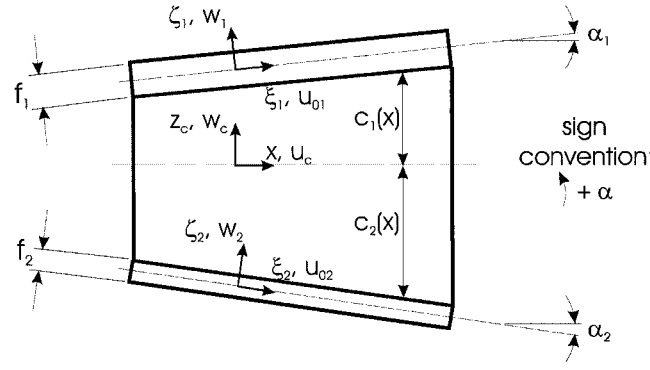

Fig. 1 Geometrical definition of variable core thickness (tapered) sandwich panels.

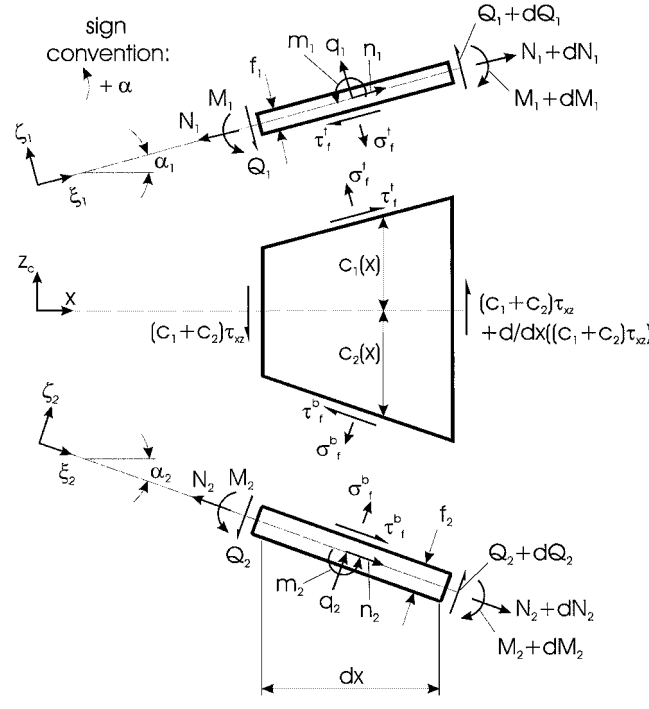

Fig. 2 Equilibrium elements of tapered sandwich panel.

the existence of transverse normal stresses in the core material is accounted for.

The face displacement components are denoted by u_i and w_i, $i = 1, 2$, and are defined relative to the local face coordinate systems, ξ_i and ζ_i in Fig. 2. The core displacement components u_c and w_c, are defined relative to the core coordinates x and z_c (Fig. 2).

The adopted high-order sandwich formulation is equivalent to the high-order sandwich formulations originally introduced for the analysis of flat sandwich panels by Frostig et al.[9] Frostig and Shenar,[10] and Frostig and Baruch[11]; for the analysis of tapered sandwich panels by Peled and Frostig[12] and Frostig and Peled[13]; for the analysis of adhesive bonded joints by Frostig et al.[14]; for the analysis of multilayer-sandwich-type structures by Thomsen[15,16]; and recently for the analysis of sandwich aircraft fuselage structures by Thomsen and Vinson.[5,6] In the present study, however, the high-order sandwich formulation is extended, compared to Refs. 5 and 9–16, to include bending–stretching coupling and transverse shear effects in the face sheets. These effects have proven to be important in some cases of sandwich panels with laminated composite face sheets and soft/compliant cores.[6] The reason is that the localized bending and shearing effects can play an important role in such structures, where the mechanical behavior of the face sheets is highly determined by the bending–stretching coupling and transverse shear properties.[6] Thus, the buildup of localized stress concentrations due to localized bending is highly influenced by the stiffness properties of the face sheets.

As mentioned, the high-order model adopted in the present paper includes the transverse flexibility of the core and, therefore, allows the face sheets to deflect differently under the action of external loading. This makes it possible to quantify and evaluate the localized bending effects, as well as the overall bending and shearing action effects. Note however, that because the faces are modeled using a beam/plate/shell formulation the model does not provide very accurate information about the local stress concentrations in the faces in the vicinity of load introductions, support points, and locations of abrupt changes of geometry. The weak point in such structures, however, is the core/face interfaces or the core itself in the vicinity of discontinuities as already mentioned. Experimental results,[17] as well as comparisons with exact elasticity solutions for rectangular sandwich plates with composite faces,[18] have shown that the interface and core stresses are predicted reasonably accurately by the high-order sandwich theory models. Moreover, to obtain more accurate results, it is necessary to apply much more complex analytical models, or alternatively to conduct elaborate finite element analyses with solid elements and very fine mesh densities.

Kassapoglu,[8] in principle, applied the same basic concepts as presented in Refs. 5 and 6 and 9–16. Thus, in Ref. 8, a similar continuum formulation for the core material is adopted, and the faces are modeled individually as laminated beams or plates. However, the analysis presented in Ref. 8 is focused entirely on the solution of the rampdown problem in sandwich panels, and a general high-order sandwich beam or plate theory is not derived.

Core Stress and Displacement Fields

To include the transverse core flexibility, the core material is modeled as a special type of orthotropic linear elastic solid only possessing stiffness in the out-of-plane direction. Consequently, the core stiffness is characterized exclusively by the transverse Young's modulus E_c and the transverse shear modulus G_c. Because of the zero in-plane stiffness, the in-plane normal stress is nil, and the stress field is defined solely by the transverse normal stress σ_z, and the shear stress τ_{xz}.

The response of the core material is coupled with the responses of the face sheets by requiring continuity of the displacements across the core/face boundaries, that is, at $z_c = c_1(x)$ and $z_c = -c_2(x)$ (Fig. 1).

The lengthwise variation of the core thickness $c[c = c(x)]$ is defined relative to the core reference plane (which can be chosen arbitrarily) according to the following linear relationships:

$$c_1(x) = c_1^0 + \delta_1 x, \qquad \delta_1 = \left(c_1^{\text{end}} - c_1^0\right)/L$$

$$c_2(x) = c_2^0 + \delta_2 x, \qquad \delta_2 = \left(c_2^{\text{end}} - c_2^0\right)/L$$

$$c(x) = c_1(x) + c_2(x) \tag{1}$$

where $c_1^0 + c_2^0 = c_0$ (c_0 is the initial core thickness), $c_1^{\text{end}} + c_2^{\text{end}} = c_e$ (c_e is the final core thickness), and δ_i, $i = 1, 2$, are the slopes of the upper and lower face sheets, respectively.

When the equilibrium, the kinematic, and the constitutive relations are utilized for the core material considered as a two-dimensional elastic continuum, together with the assumption of zero in-plane core stiffness, and with the conditions of continuity of displacements across the core/face boundaries, the following closed-form expressions for the core stress and displacement fields can be derived:

$$\tau_{xz}(x, z) = \tau_{xz}(x)$$

$$\begin{aligned}\sigma_z(x, z) = {} & [E_c/c(x)]\{u_1(\xi_1, -f_1/2)\sin\alpha_1 + w_1(\xi_1)\cos\alpha_1 \\ & - u_2(\xi_2, f_2/2)\sin\alpha_2 - w_2(\xi_2)\cos\alpha_2\} \\ & - \tau_{xz,x}\{z - [c_1(x) - c_2(x)]/2\}\end{aligned}$$

$$\begin{aligned}w_c(x, z) = {} & -(\tau_{xz,x}/2E_c)\left\{z^2 - [c_1(x) - c_2(x)]z - c_1(x)c_2(x)\right\} \\ & + u_1(\xi_1, -f_1/2)\sin\alpha_1 + w_1(\xi_1)\cos\alpha_1 + \{u_1(\xi_1, -f_1/2)\sin\alpha_1 \\ & + w_1(\xi_1)\cos\alpha - u_2(\xi_2, f_2/2)\sin\alpha \\ & - w_2(\xi_2)\cos\alpha_2\}[z - c_1(x)]/c(x)\end{aligned}$$

$$\begin{aligned}u_c(x, z) = {} & u_{01}\langle\cos\alpha_1 - \sin\alpha_1\chi_1(x, z)\rangle + u_{01,x}\sin\alpha_1\chi_2(x, z) \\ & - w_1\langle\sin\alpha_1 + \cos\alpha_1\chi_1(x, z)\rangle + w_{1,x}\langle(f_1/2)\{\cos\alpha_1 \\ & - \sin\alpha_1\chi_1(x, z)\} + \cos\alpha_1\chi_2(x, z)\rangle + w_{1,xx}(f_1/2) \\ & \times \sin\alpha_1\chi_2(x, z) - (Q_1 f_1)/\left(2C_{55}^1\right)\langle\cos\alpha_1 - \sin\alpha_1\chi_1(x, z)\rangle \\ & - (Q_{1,x} f_1)/\left(2C_{55}^1\right)\sin\alpha_1\chi_2(x, z) + u_{02}\sin\alpha_2\chi_1(x, z) \\ & - u_{02,x}\sin\alpha_2\chi_3(x, z) + w_2\cos\alpha_2\chi_1(x, z) - w_{2,x}\langle(f_2/2) \\ & \times \sin\alpha_2\chi_1(x, z) + \cos\alpha_2\chi_3(x, z)\rangle + w_{2,xx}(f_2/2) \\ & \times \sin\alpha_2\chi_3(x, z) + (Q_2 f_2)/\left(2C_{55}^2\right)\sin\alpha_2\chi_1(x, z) \\ & - (Q_{2,x} f_2)/\left(2C_{55}^2\right)\sin\alpha_2\chi_3(x, z) - (\tau_{xz}/G_c)\langle c_1(x) - z\rangle \\ & + \tau_{xz,x}\chi_4(x, z) - \tau_{xz,xx}\chi_5(x, z)\end{aligned} \tag{2}$$

where C_{55}^i, $i = 1, 2$, is the transverse shear stiffness of the faces, β_i, $i = 1, 2$, is the rotation of the normals to the midlines of the faces, and

$$\begin{aligned}\chi_1(x, z) = {} & [1/c(x)^2]\left\langle(\delta_1 + \delta_2)\left[c_1(x)^2/2 - z^2/2\right]\right. \\ & \left. + [\delta_1 c_2(x) - \delta_2 c_1(x)][c_1(x) - z]\right\rangle\end{aligned}$$

$$\chi_2(x, z) = [c_1(x) - z] - [1/c(x)]\left\langle z^2/2 + c_1(x)^2/2 - c_1(x)z\right\rangle$$

$$\chi_3(x, z) = \chi_2(x, z) - [c_1(x) - z]$$

$$\begin{aligned}\chi_4(x, z) = {} & (1/2E_c)\left\langle\left\langle(\delta_1 - \delta_2)\left[c_1(x)^2/2 - z^2/2\right]\right.\right. \\ & \left.\left. + \left(\delta_2 c_1^0 + \delta_1 c_2^0 + 2\delta_1\delta_2 x\right)[c_1(x) - z]\right\rangle\end{aligned}$$

$$\begin{aligned}\chi_5(x, z) = {} & (1/2E_c)\left\langle c_1(x)^3/3 - z^3/3 - [c_1(x) - c_2(x)]\left[c_1(x)^2/2\right.\right. \\ & \left.\left. - z^2/2\right] - c_1(x)c_2(x)[c_1(x) - z]\right\rangle\end{aligned} \tag{3}$$

It is seen from Eqs. (2) and (3) that τ_{xz} is predicted to be constant, that σ_z varies linearly, that w_c varies quadratically, and that u_c varies cubically across the core thickness.

Governing Equations for the Faces

The faces are modeled using classical lamination theory as laminated beams or plates with inclusion of bending–stretching coupling effects as well as transverse shear effects. Thus, the modeling of the faces corresponds to a first-order shear approach. Dissimilar faces, that is, faces of different materials, different laminate stacking sequences, and different thicknesses, can be included in the analysis.

Figure 2 shows the equilibrium elements of the tapered sandwich panel element shown in Fig. 1.

When Figs. 1 and 2 are referred to, the face beam constitutive relations in the straight, tapered, and curved panel sections read

$$N_i = A_{11}^i\varepsilon_{0i} + B_{11}^i\kappa_i, \qquad M_i = B_{11}^i\varepsilon_{0i} + D_{11}^i\kappa_i$$

$$Q_i = C_{55}^i\gamma_{\xi\varsigma i}, \qquad i = 1, 2 \tag{4}$$

where ε_{0i}, κ_i, and γ_{mni} are the midplane normal strains, the curvature change of the face sheet midlines, and the transverse shear strains. A_{11}^i, B_{11}^i, D_{11}^i, and C_{55}^i, $i = 1, 2$, are the principal face sheet extensional, coupling, bending, and transverse shear stiffnesses obtained from classical lamination theory[2]:

$$A_{11}^i = \sum_{k=1}^{\Gamma^i} \left(Q_{11}^i\right)_k (h_k - h_{k-1})$$

$$B_{11}^i = \frac{1}{2} \sum_{k=1}^{\Gamma^i} \left(Q_{11}^i\right)_k \left(h_k^2 - h_{k-1}^2\right)$$

$$D_{11}^i = \frac{1}{3} \sum_{k=1}^{\Gamma^i} \left(Q_{11}^i\right)_k \left(h_k^3 - h_{k-1}^3\right)$$

$$C_{55}^i = \frac{5}{4} \sum_{k=1}^{\Gamma^i} \left(Q_{55}^i\right)_k \left[h_k - h_{k-1} - \frac{4}{3f_i}\left(h_k^3 - k_{k-1}^3\right)\right], \qquad i = 1, 2 \tag{5}$$

where Γ^i, $i = 1, 2$, is the number of laminas in the upper and lower faces, respectively, and where

$$\left(Q_{11}^i\right)_k = \left[\frac{E_{11}^i}{\left(1 - \nu_{12}^i \nu_{21}^i\right)}\right]_k, \qquad \left(Q_{55}^i\right)_k = \left(G_{13}^i\right)_k$$

$$i = 1, 2 \tag{6}$$

In Eqs. (6), $(E_{11}^i)_k$, $(\nu_{12}^i)_k$, $(\nu_{21}^i)_k$, and $(G_{13}^i)_k$, $i = 1, 2$ and $k = 1, \ldots, \Gamma^i$, are the Young's moduli, the in-plane Poisson's ratios, and the transverse shear stiffnesses of the kth laminas of the upper and lower face laminates, respectively.

The analysis is limited to small strains and very small rotations, and accordingly the strain–displacement relations read

$$u_i = u_{0i} + \varsigma_i \beta_i, \qquad \varepsilon_i = \varepsilon_{0i} + \varsigma_i \kappa_i, \qquad \varepsilon_{0i} = u_{0i,\xi}$$

$$w_{i,\xi} = \gamma_{\xi\zeta i} - \beta_i, \qquad \kappa_i = \beta_{i,\xi}, \qquad i = 1, 2 \tag{7}$$

With reference to Fig. 2, the equilibrium equations can be expressed in the form

$$N_{1,x} \cos\alpha_1 - \sigma_z^t \cos\alpha_1 \sin\alpha_1 - \tau_{xz}\left\{\cos^2\alpha_1 - \sin^2\alpha_1\right\} + n_1 = 0$$

$$Q_{1,x} \cos\alpha_1 - \sigma_z^t \cos^2\alpha_1 + \tau_{xz} 2 \cos\alpha_1 \sin\alpha_1 + q_1 = 0$$

$$M_{1,x} \cos\alpha_1 - Q_1 + (f_1/2)\left\langle\sigma_z^t \cos\alpha_1 \sin\alpha_1 + \tau_{xz}\left\{\cos^2\alpha_1 - \sin^2\alpha_1\right\}\right\rangle - m_1 = 0$$

$$N_{2,x} \cos\alpha_2 + \sigma_z^b \cos\alpha_2 \sin\alpha_2 + \tau_{xz}\left\{\cos^2\alpha_2 - \sin^2\alpha_2\right\} + n_2 = 0$$

$$Q_{2,x} \cos\alpha_2 + \sigma_z^b \cos^2\alpha_2 - \tau_{xz} 2 \cos\alpha_2 \sin\alpha_2 + q_2 = 0$$

$$M_{2,x} \cos\alpha_2 - Q_2 + (f_2/2)\left\langle\sigma_z^b \cos\alpha_2 \sin\alpha_2 + \tau_{xz}\left\{\cos^2\alpha_2 - \sin^2\alpha_2\right\}\right\rangle - m_2 = 0 \tag{8}$$

The transformation between the face/core interface transverse normal and shear stresses defined in local face coordinates ξ_i and ζ_i and the core transverse normal and shear stresses defined in the core coordinates x and z_c (Fig. 1) is carried out according to the following expressions:

$$\tau_f^i = \sigma_z^i \cos\alpha_j \sin\alpha_j + \tau_{xz}\left\{\cos^2\alpha_j - \sin^2\alpha_j\right\}$$

$$\sigma_f^i = \sigma_z^i \cos^2\alpha_j - 2\tau_{xz} \cos\alpha_j \sin\alpha_j$$

$$i = t, b, \qquad j = 1, 2 \tag{9}$$

In Eqs. (8) and (9), note that the inclination angles α_j, $j = 1, 2$, are considered positive in the counterclockwise direction (Figs. 1 and 2). Also in Eqs. (8) and (9), n_i, q_i, and m_i, $i = 1, 2$, are distributed in-plane, lateral, and bending moment loads. Superscripts t and b refer to the top and bottom core/face boundaries, respectively.

Governing Equations and Boundary Conditions

When the face sheet equations (4–9) are combined with the core layer equations (5–9), and displacement continuity is imposed across the core/face boundaries, the set of governing differential equations is obtained. The governing equations can be represented in the general form of 14 coupled first-order ordinary differential equations:

$$\frac{\mathrm{d}}{\mathrm{d}s}\{y(x)\} = [A(x)]\{y(x)\} + \{B(x)\}$$

$$\{y(x)\} = \{u_{01}, w_1, \beta_1, N_1, M_1, Q_1, \tau_{xz}, \tau_{xz,x}, u_{02}, w_2, \beta_2, N_2, M_2, Q_2\} \tag{10}$$

In Eqs. (4), $\{y(x)\}$ is the vector of fundamental variables, $[A(x)]$ is a stiffness matrix, and $\{B(x)\}$ is a vector of nonhomogeneous load terms.

The order of the set of governing equations is 14, and consequently, the number of boundary conditions to be specified on an edge $x = \text{const}$ is $\frac{14}{2} = 7$, three for each face and one for the core material.

The governing equations together with the boundary conditions constitute a boundary-value problem, which in the present case was solved numerically using the multiple point shooting method described in Ref. 19 and used recently in Refs. 5, 6, 15, and 16.

Comparison with Finite Element Results and Numerical Examples

To illustrate the features of the load transfer mechanisms in sandwich panels with varying core thickness, as well as to demonstrate the applicability of the developed high-order sandwich theory formulation, the results of a numerical study will be presented. For simplicity, the case of a sandwich panel in three-point bending has been chosen, and the two different sandwich panel configurations shown in Fig. 3 are analyzed.

Example A is a sandwich beam with a continuous taper. Example B is a sandwich beam with three sections, two flat sections next to the simple supports at the ends and one tapered section in the middle of the beam.

Specification of Boundary Conditions

With reference to Fig. 3, the boundary and continuity conditions for the two sandwich beam configurations are prescribed as follows:

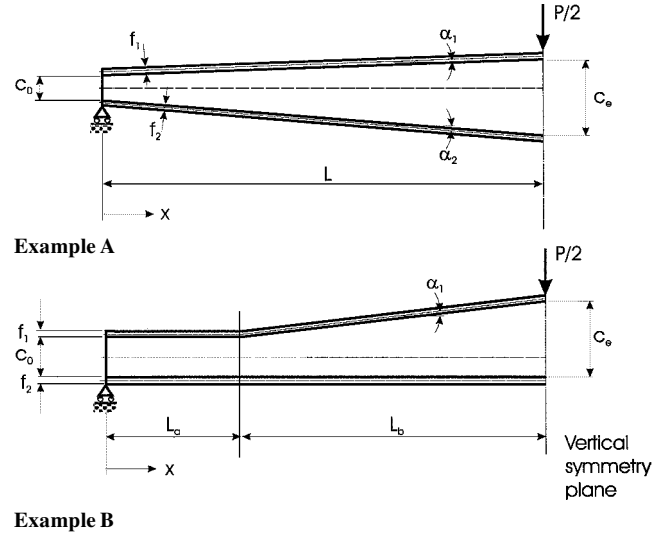

Fig. 3 Tapered sandwich panel configurations in three-point bending. (Only one half is shown due to symmetry.)

Example A: Continuous Taper

With simple (rolling) horizontal support at $x = 0$,

$$N_1 \cos\alpha_1 - Q_1 \sin\alpha_1 = 0, \qquad N_1 \sin\alpha_1 + Q_1 \cos\alpha_1 = 0$$
$$M_1 = 0, \qquad \tau_{xz} = 0, \qquad u_2 \cos\alpha_2 - w_2 \sin\alpha_2 = 0$$
$$u_2 \sin\alpha_2 + w_2 \cos\alpha_2 = 0, \qquad M_2 = 0 \tag{11}$$

With the vertical plane of symmetry at $x = L$,

$$u_1 \cos\alpha_1 - w_1 \sin\alpha_1 = 0, \qquad N_1 \sin\alpha_1 + Q_1 \cos\alpha_1 = -P/2$$
$$\beta_1 = 0, \qquad \tau_{xz} = 0, \qquad u_2 \cos\alpha_2 - w_2 \sin\alpha_2 = 0$$
$$N_2 \sin\alpha_2 + Q_2 \cos\alpha_2 = 0, \qquad \beta_2 = 0 \tag{12}$$

Example B: Flat and Tapered Sections

With simple (rolling) support conditions at $x = 0$,

$$N_1 = M_1 = Q_1 = 0, \qquad \tau_c = 0, \qquad w_2 = N_2 = M_2 = 0 \tag{13}$$

There is a junction between the flat and tapered part of the sandwich panel and continuity of the fundamental variables, that is,

$$u_{0i}^{+} = u_{0i}^{-} \cos\alpha_i + w_i^{-} \sin\alpha_i, \qquad w_i^{+} = -u_{0i}^{-} \sin\alpha_i + w_i^{-} \cos\alpha_i$$
$$\beta_i^{+} = \beta_i^{-}, \qquad N_i^{+} = N_i^{-} \cos\alpha_i + Q_i^{-} \sin\alpha_i, \qquad M_i^{+} = M_i^{-}$$
$$Q_i^{+} = -N_i^{-} \sin\alpha_i + Q_i^{-} \cos\alpha_i, \qquad \tau_{xz}^{+} = \tau_{xz}^{-}$$
$$\tau_{xz,x}^{+} = \tau_{xz,x}^{-}, \qquad i = 1, 2 \tag{14}$$

In Eqs. (14) superscripts + and − refer to the values of the fundamental variables when the junction is approached from the left and the right sides, respectively.

In the vertical plane of symmetry,

$$u_1 \cos\alpha_1 - w_1 \sin\alpha_1 = 0, \qquad N_1 \sin\alpha_1 + Q_1 \cos\alpha_1 = -P/2$$
$$\beta_1 = 0, \qquad \tau_{xz} = 0, \qquad u_2 \cos\alpha_2 - w_2 \sin\alpha_2 = 0$$
$$N_2 \sin\alpha_2 + Q_2 \cos\alpha_2 = 0, \qquad \beta_2 = 0 \tag{15}$$

For both examples A and B, the distributed surface loads are given by

$$n_1 = q_1 = m_1 = 0, \qquad n_2 = m_2 = q_2 = 0 \tag{16}$$

Geometry, Material Properties, and External Load

The constituent materials are assumed to be carbon/epoxy T300/5208 unidirectional for both face sheets, together with a polymeric foam core. The material data are assumed to be as follows:

For the foam core, $E_c = 100$ MPa, and $G_c = 38.5$ MPa (Klegecell PVC foam, density 100 kg/m^3). For the face sheets, $E_{11} = 153.0$ GPa, $G_{13} = 5.6$ GPa, $\nu_{13} = 0.3$, and $\nu_{31} = 0.021$.

The geometry of the two sandwich beam examples is defined by the following: For example A, symmetric with continuous taper, $L = 1000$ mm, $c_0 = 200$ mm, $c_e = 300$ mm, $f_1 = f_2 = 5$ mm, and $\tan\alpha_1 = -\tan\alpha_2 = 0.05$ ($\alpha_1 = -\alpha_2 \approx 2.9$ deg). For example B, flat and tapered configuration, $L_a = L_b = 500$ mm, $c_0 = 200$ mm, $c_e = 300$ mm, $f_1 = f_2 = 5$ mm, $\tan\alpha_1 = 0.2$, and $\tan\alpha_2 = 0$ ($\alpha_1 \approx 11.3$ deg, $\alpha_2 = 0$). The external point load is defined per unit width of the sandwich beam, $P = 100$ N/mm.

Sandwich Configuration A: Comparison with Finite Element Analysis Results

Comparative finite element analyses have been conducted with the objective of validating the developed high-order sandwich theory for sandwich beams and plates with varying core thickness. For the purposes of the present paper, selected comparative results obtained for sandwich panel configuration A (symmetric and with a continuous taper) are presented.

The finite element analysis was performed using a four-node MITC[20]-stabilized general shell element implemented in the software package MUST developed at the Institute of Mechanical Engineering, Aalborg University.[20] The element has five degrees of freedom (DOF) per node, but all out-of-plane DOF have been restrained in the analysis to enforce the two-dimensional conditions of the high-order sandwich theory. Thus, the general shell element was used as a pure membrane element.

The tapered sandwich panel (example A) was modeled using 10 elements through the thickness of each face sheet and 40 elements through the thickness of the core. In all, 15,000 elements and 15.311 nodes have been used for the model. Only one-half of the tapered sandwich panel was modeled, and the boundary conditions of the finite element model were adopted from the high-order sandwich beam/plate model.

Figure 4a shows one-half of the tapered sandwich panel as predicted by the finite element analysis. The meshing of the finite element model is also shown in Fig. 4, and the contours shown represent the predicted lateral displacements.

Figure 4b also shows the vertical displacements of the midplanes of the top and bottom faces and the core, as predicted by the high-order sandwich theory HOST and the finite element analysis (FEA). The displacement patterns obtained from the two methods generally compare very well. It is seen, however, that the FEA results are slightly lower than the HOST results, which can be attributed to that the finite element method generally exaggerates the stiffness of the structure. The peak lateral displacement occurs at the top face at the vertical midplane and is predicted as 6.3 mm (w_1^{HOST}) by the HOST analysis, whereas it is predicted at 5.8 mm by FEA (w_1^{FEA}). A characteristic nontrivial feature of the displacement patterns predicted

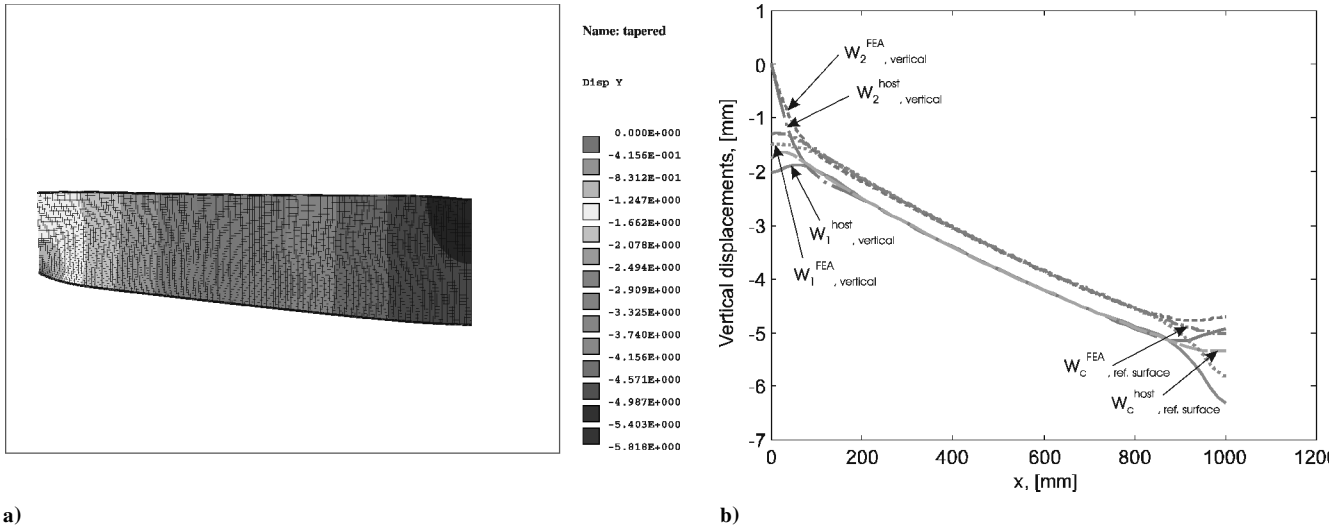

Fig. 4 Deformed finite element model and comparison of vertical displacements predicted by HOST and FEA.

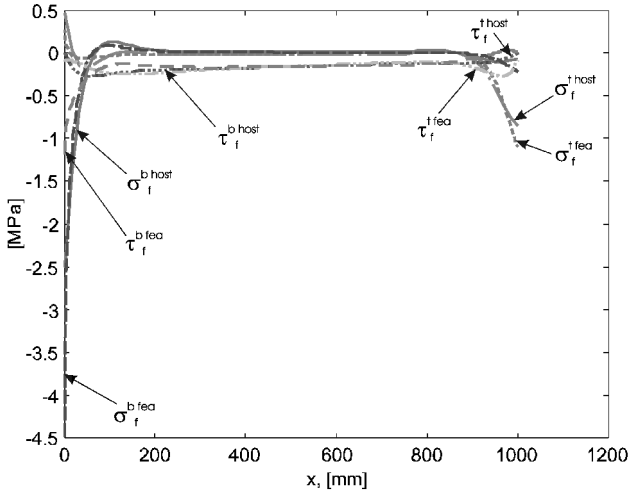

a) Core stresses at core/face boundaries

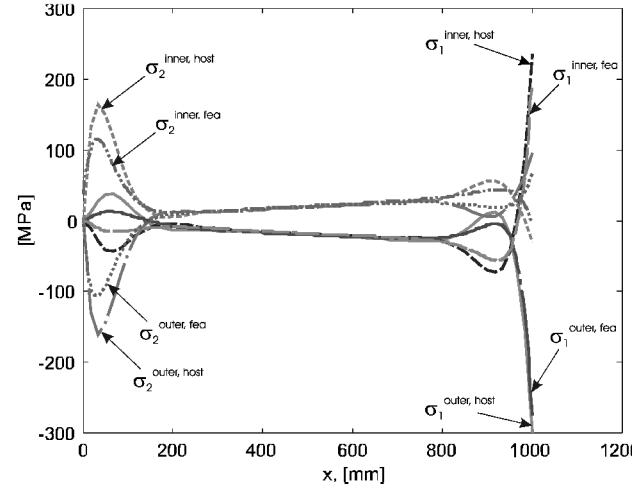

b) Face stresses

Fig. 5 Comparison between HOST and FEA results.

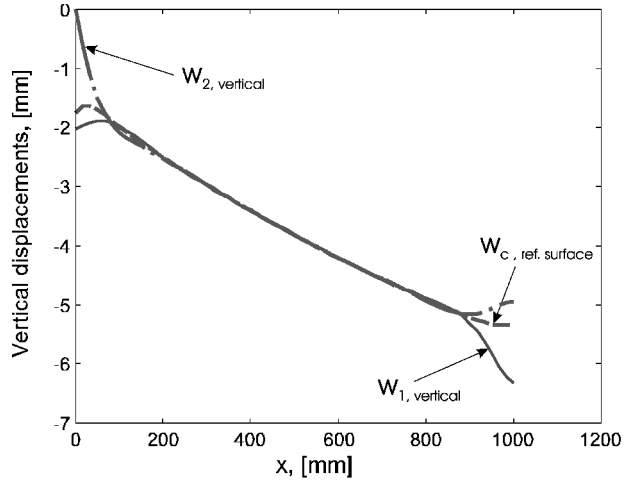

Example A

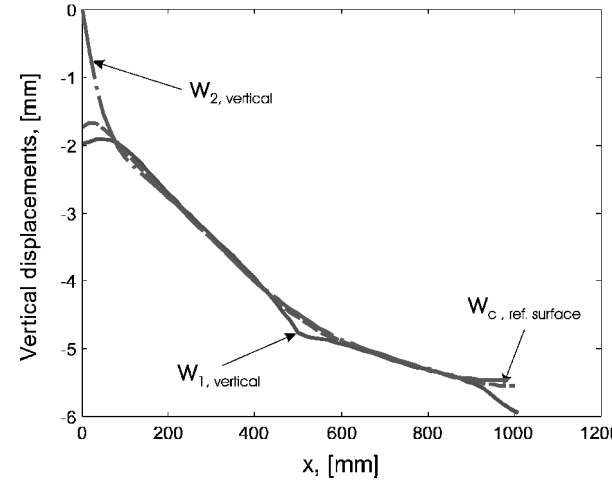

Example B

Fig. 6 Vertical displacement components.

by both methods is that the lower face tends to bulge upward locally in the vicinity of the vertical midplane of the sandwich panel. This behavior is somewhat counterintuitive and cannot be predicted by application of simpler classical sandwich or beam theories, as described in Refs. 1 and 2, for example.

Figure 5 shows the distributions of the core stresses at the core face/interfaces and the face normal stresses predicted by HOST and FEA, respectively.

Figure 5a shows the core stresses at the top and bottom face/core interfaces. The stresses are given in the local face coordinates. (See Fig. 3 for definition of the stresses σ_f^t, σ_f^b, τ_f^t, and τ_f^b.) The detailed features of the predicted core stress distributions will be discussed later, but it is seen from Fig. 5 that the overall patterns predicted by HOST and FEA are very similar. The numerical values predicted also match very well at the vertical plane of symmetry and in the interior parts of the sandwich panel. At the left end, that is, in the vicinity of the rolling support (Fig. 3), the match is less convincing with respect to the predicted numerical values even though the overall distribution patterns are similar. The observed discrepancy is especially pronounced with respect to the predicted values of the transverse normal stresses at the lower core/face interface exactly at the position of the rolling support (compressive peak values): $(\sigma_f^t)^{\text{HOST}} \approx -2.5$ MPa, whereas $(\sigma_f^t)^{\text{FEA}} \approx -4.5$ MPa. The cause of this discrepancy is not clear, but note that neither of the methods can be expected to provide very accurate results exactly at the point of contact between the support and the lower face.

Figure 5b shows the face stresses predicted by the two methods in the inner and outer fibers of the top and bottom faces, respectively. (Here σ_i^{inner} and σ_1^{outer} are the normal stresses in the inner and outer fibers of the top face, respectively, and σ_2^{inner} and σ_2^{outer} are the normal stresses in the inner and outer fibers of the bottom face sheet.) As for the core stresses, the detailed features of the predicted face stress distributions will be discussed later, but it is seen from Fig. 5 that both the overall distribution patterns as well as the actual numerical values predicted by HOST and FEA display a close match. Thus, the two methods agree with respect to the quantitative description of both the overall and the localized bending phenomena that are active in the chosen example.

In conclusion, it can be stated that the HOST and the FEA have provided very similar results, with respect to both the overall distribution features and the actual numerical values.

Numerical Results: Comparison of Sandwich Configurations A and B

The two cases of tapered sandwich panels shown in Fig. 3 will be compared in some detail. The numerical results have been derived using HOST as presented in this paper. Selected results will be presented, and important features of the elastic response of the two sandwich panel configurations will be compared.

Figure 6 shows the vertical displacement components of the faces and of the reference plane of the core material. From Fig. 6 it is seen that configuration B is stiffer than configuration A in a global sense because the peak deflections are lower. It is also observed that significant local bending effects are present in the vicinity of the support point, $x = 0$, and the load application point, $x = 1000$ mm. In these regions, it is seen that the sandwich panel thickness changes significantly due to indentation of either the bottom, $x = 0$, or the

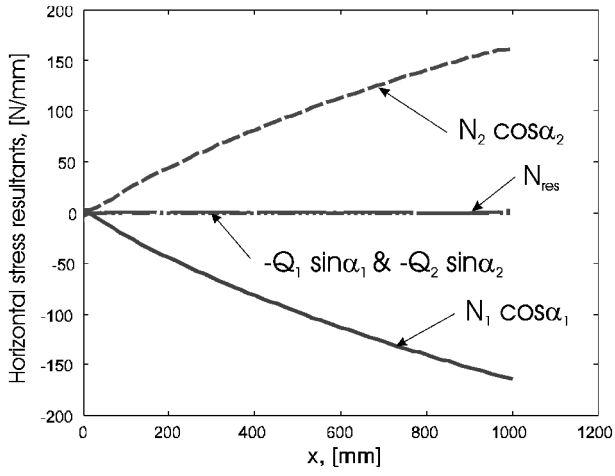

Example A

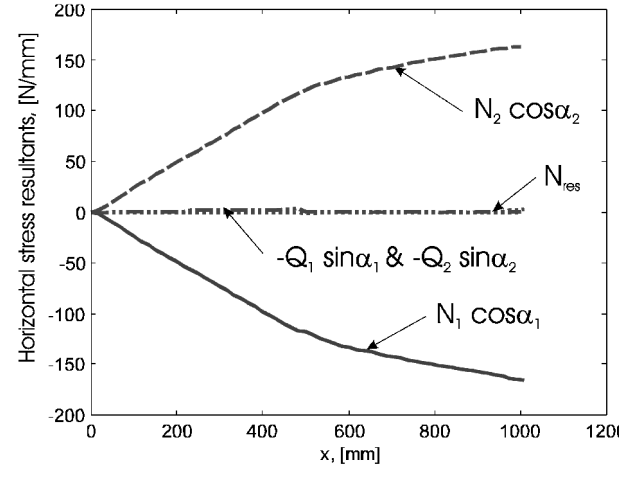

Example B

Fig. 7 Horizontal stress resultants.

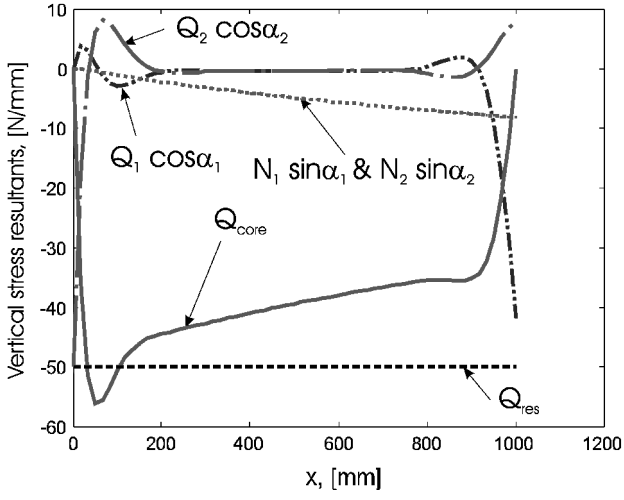

Example A

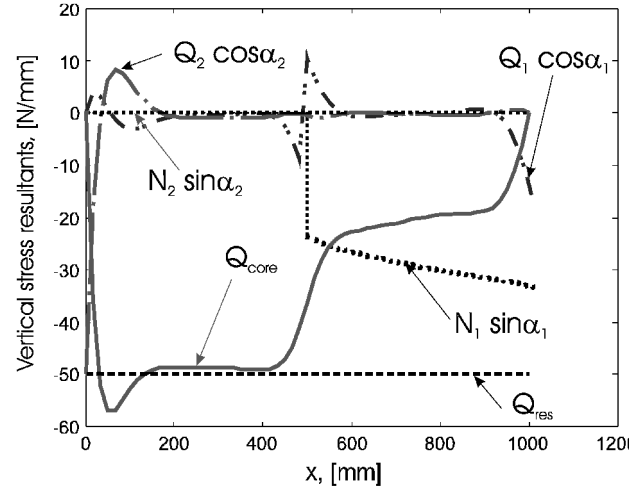

Example B

Fig. 8 Vertical stress resultants.

top face into the core material, $x = 1000$ mm. For example B, it is also seen that local bending effects occur in the vicinity of the junction between the flat and the tapered sections at $x = 500$ mm.

Figure 7 shows the distribution of horizontal stress resultants in the faces and the core material. It is observed that the primary contributions to the horizontal stress resultants stem from the in-plane face resultants N_1 and N_2. Also, it is seen that there is no net horizontal stress resultant as expected due to the simple support conditions adopted.

Figure 8 shows the distribution of vertical stress resultants in the faces and the core material. It is seen that the overall distribution pattern is complicated and that all of the stress resultants contribute significantly to the vertical load transfer for both examples A and B. When example A is considered, it is observed that the vertical component of the in-plane normal stress resultants contribute significantly despite the relatively modest taper ($\alpha_1 = -\alpha_2 \approx 2.9$ deg) of the sandwich beam. However, the vertical resultant of the core shear stresses Q_{core} contributes most significantly to the overall shear load transfer, as expected. When example B is considered, it is seen that the vertical load transfer changes significantly at the junction between the flat and the tapered beam sections. Thus, in the flat beam section, the in-plane stress resultants do not contribute at all, because they do not have a vertical component, whereas N_1 and N_2 contribute significantly to the overall shear load transfer in the tapered zone of the beam. This observation is, in fact, the key to understanding the principal difference between the load transfer mechanisms in laterally loaded flat and tapered sandwich beams. Thus, it is seen that the core shear stresses (and, thereby, the core shear stress resultant Q_{core}) are relieved considerably in the tapered section because of the increased shear load transfer capability of the faces in this zone. As expected for the three-point beam bending problem, it is observed that the total resultant of the transverse shear stress resultants Q_{res} is constant ($Q_{\text{res}} = -P/2 = -50$ N/mm) along the length of the beam.

Figure 9 shows the distribution of the bending moment resultants for examples A and B. It is seen that the local face bending moment resultants M_1 and M_2 are of very modest magnitude, compared to the resulting bending moment resultant M_{res}. As expected for the three-point beam bending problem, it is also observed that M_{res} varies linearly along the beam length.

Figure 10 shows the core stresses along the interfaces between the core material and the faces. (See Fig. 3 for definition of the stresses σ_f^t, σ_f^b, τ_f^t, and τ_f^b.) It is seen that the results for the two examples are very similar. Considering the transverse normal stress distributions, it is seen that very high compressive stress peaks are present at the lower face/core interface at $x = 0$ (support point).

In Fig. 10 it is also seen that compressive stress peaks of significantly smaller magnitude are present at the upper face/core interface at the beam midspan, $x = 1000$ mm. These compressive stress peaks correspond to the local indentations of the bottom and upper faces displayed in Fig. 6. It is further observed that the peak value of σ_f^t (interface normal stress at top interface) at $x = 1000$ mm is significantly lower for example B than for example A. The reason for this is that the taper angle of the top face sheet is much larger for example B than for example A. This increases the shear load transfer capability of the top face in example B considerably, and a smaller

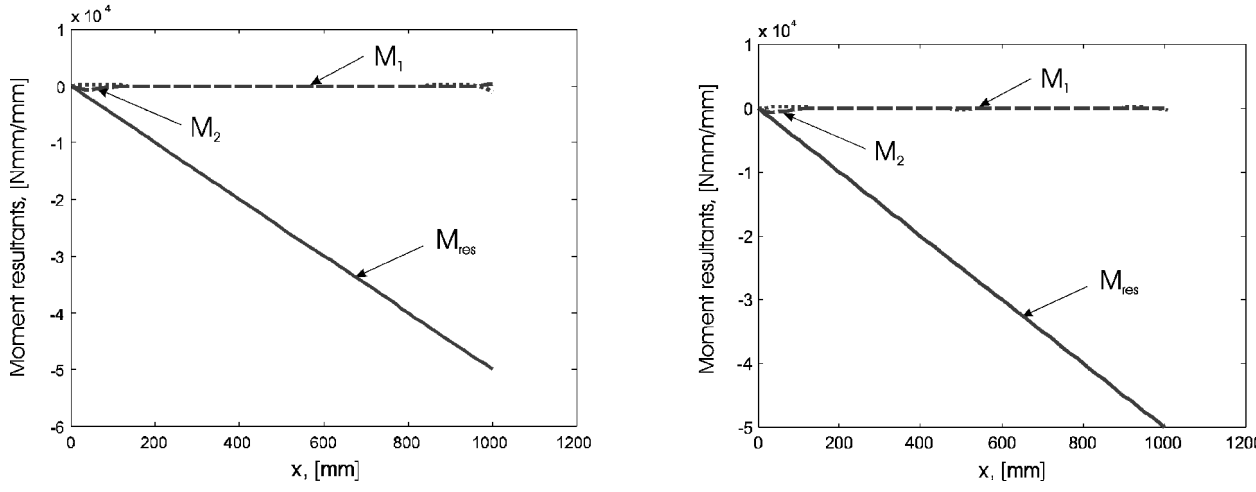

Example A **Example B**

Fig. 9 Bending moment resultants.

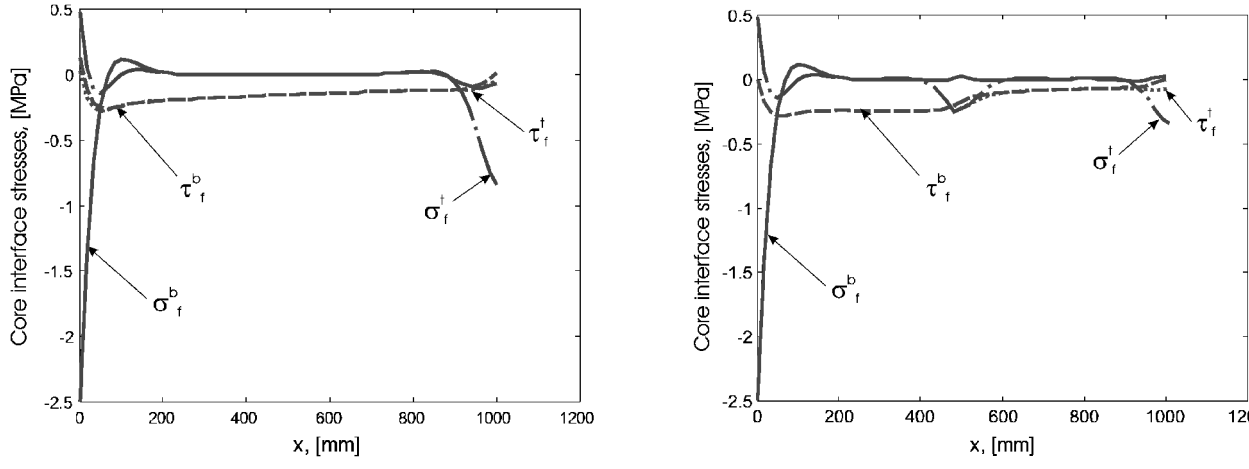

Example A **Example B**

Fig. 10 Core stresses at face/core boundaries.

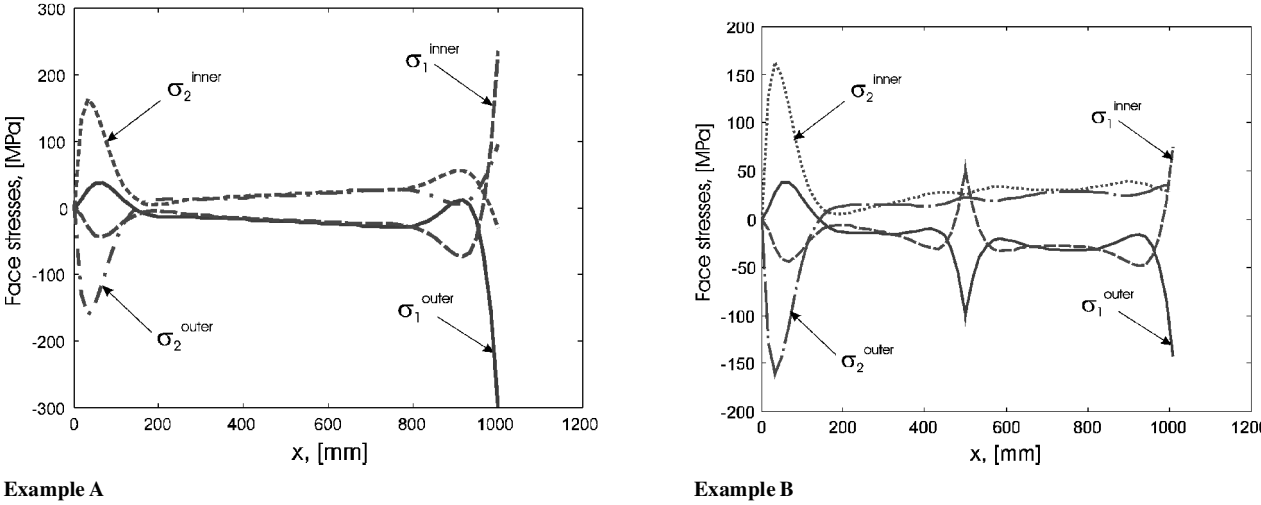

Example A **Example B**

Fig. 11 Face stresses.

amount of the applied load is thereby transferred directly into the core material.

Finally, Fig. 11 shows the normal stresses in the faces of the two sandwich panel configurations. In Fig. 9, σ_1^{inner} and σ_1^{outer} represent the normal stresses in the inner and outer fibers of the top face, respectively. Similarly, σ_2^{inner} and σ_2^{outer} represent the normal stresses in the inner and outer fibers of the bottom face sheet. As also observed from Figs. 6, 8, and 10, it is seen from Fig. 11 that significant local bending effects are present in the faces in the vicinity of the support and load application points. Thus, local stress peaks (both compressive and tensile) of very high magnitude are induced at these locations. Between the support point, $x = 0$, and the load application point, $x = 1000$ mm, the face stresses display a linear variation with compression in the bottom and tension in the upper face. This pattern corresponds exactly to the magnitude and distribution of the total bending moment resultant M_{res} shown in Fig. 9. However, the

local bending moment resultants M_1 and M_2, although numerically small compared with M_{res} (Fig. 9), increase sufficiently in the end and midspan zones to induce the significant localized stress peaks shown in Fig. 11. When example A is compared to example B, it is seen that the local stress peaks induced at $x = 1000$ mm (midspan) are much smaller for the latter. The reason for this is that taper angle of the top face is much steeper for example B than for example A and, thus, provides for a much more efficient load introduction path.

Conclusions

A newly developed HOST formulation for the analysis of sandwich panels with varying core thickness and with nonparallel faces (both faces can be inclined relative to the sandwich panel reference surface) has been presented. In this formulation, the elastic response of each face is accounted for individually, including bending–coupling and transverse shear effects. The core material is modeled as a special type of orthotropic solid possessing stiffness only in the through-thickness direction. Consequently, the model includes the transverse flexibility of the core material, and the sandwich panel thickness can change during deformation.

To demonstrate the capability and the characteristics of the developed HOST formulation, two different sandwich beams in three-point bending have been analyzed: one with a continuous and symmetric taper and the other with combined flat and tapered asymmetric regions.

The results obtained for the continuous taper sandwich beam problem were compared with results obtained from an elaborate FEA. The comparison demonstrated a close match between the results obtained using the two methods.

With respect to the comparison between the continuous and symmetric tapered sandwich panel and the combined section asymmetric sandwich panel, the results of the analyses have shown that the faces interact through the core material in a very complicated way. This is especially the case in the vicinity of the load introduction and support points, as well as in the vicinity of locations of abrupt geometric change, where severe localized bending effects are induced. These localized bending effects induce severe stress concentrations in the core material as well as in the faces. In particular, the core stress state is dominated by severe transverse normal stresses in regions where the localized bending of the faces occurs. Furthermore, the analyses have demonstrated that the face normal stresses induced by localized bending can be very large, and in the two analyzed examples, these local stress peaks by far exceed the face stresses induced by overall beam bending. The local stress peaks may severely endanger the structural integrity of the sandwich panels under consideration.

Finally, the analyses have demonstrated quantitatively that the principal difference between the load transfer mechanisms in laterally loaded flat and tapered sandwich beams is that the faces in tapered sandwich panels can contribute significantly to the overall shear load transfer. This will cause a relief of the core shear stresses, and the effect may be significant even for relatively small taper angles.

Acknowledgments

The work presented in this paper was cosponsored by the Danish Research Councils under the "Program on Materials Research" and by the U.S. Navy, Office of Naval Research (ONR) under Grant/Award N00014001034, "Research in Advanced Composite Sandwich Constructions for Naval Surface Vessels: Analysis, Design and Optimization of Sandwich Shells." The ONR supervisor was Yapa Rajapakse. The authors acknowledge with gratitude the financial support received. The finite element analyses carried out were done by Jan Stegmann and Erik Lund, both with the Institute of Mechanical Engineering at Aalborg University. Their assistance in this matter is greatly appreciated.

References

[1]Zenkert, D., *An Introduction to Sandwich Construction*, Chameleon, London, 1995.

[2]Vinson, J. R., *The Behavior of Sandwich Structures of Sandwich Structures of Isotropic and Composite Materials*, Technomic, Lancaster, PA, 1999.

[3]Thomsen, O. T., "Localised Loads," *The Handbook of Sandwich Construction*, edited by D. Zenkert, Chameleon, London, 1997, Chap. 8, pp. 181–209.

[4]Thomsen, O. T., "Theoretical and Experimental Investigation of Local Bending Effects in Sandwich Plates," *Composite Structures*, Vol. 30, No. 1, 1995, pp. 85–101.

[5]Thomsen, O. T., and Vinson, J. R., "Analysis and Parametric Study of Non-Circular Pressurized Sandwich Fuselage Cross Section Using a High-Order Sandwich Theory Formulation," *Journal of Sandwich Structures and Materials*, Vol. 3, No. 3, 2001, pp. 220–250.

[6]Thomsen, O. T., and Vinson, J. R., "Conceptual Design Principles for Non-Circular Pressurized Sandwich Fuselage Sections—A Design Study Based on a High-Order Sandwich Theory Formulation," *Journal of Composite Materials*, Vol. 36, No. 3, 2001, pp. 313–346.

[7]Skvortsov, V., Bozhevolnaya, E., Thomsen, O. T., Lyckegaard, A., and Vinson, J. R., "Closed-Form Estimation of the Stress-Strain State at the Junctions between Curved and Straight Sandwich Panels," *Journal of Sandwich Structures and Materials* (to be published).

[8]Kassapoglou, C., "Stress Determination and Core Failure Analysis in Sandwich Rampdown Structures under Bending Loads," *Key Engineering Materials*, Vol. 120–121, 1996, pp. 307–328.

[9]Frostig, Y., Baruch, M., Vilnai, O., and Sheinman, I., "High-Order Theory for Sandwich Beam Bending with Transversely Flexible Core," *Journal of Engineering Mechanics*, Vol. 118, 1992, pp. 1026–1043.

[10]Frostig, Y., and Shenhar, Y., "High-Order Bending of Sandwich Beams with a Transversely Flexible Core and Unsymmetrical Laminated Composite Skins," *Composites Engineering*, Vol. 5, 1995, pp. 405–414.

[11]Frostig, Y., and Baruch, M., "Localized Load Effects in High-Order Bending of Sandwich Panels with Transversely Flexible Core," *Journal of Engineering Mechanics*, Vol. 122, No. 11, 1996.

[12]Peled, D., and Frostig, Y., "High-Order Bending of Sandwich Beams with Transversely Flexible Core and Nonparallel Skins," *Journal of Engineering Mechanics*, Vol. 120, No. 6, 1994, pp. 1255–1269.

[13]Frostig, Y., and Peled, D., "High-Order Bending of Piecewise Uniform Sandwich Beams with a Tapered Transition Zone and a Transversely Flexible Core," *Composite Structures*, Vol. 31, 1995, pp. 151–162.

[14]Frostig, Y., Thomsen, O. T., and Mortensen, F., "Analysis of Adhesive-Bonded Joints, Square-End and Spew-Fillet—High-Order Theory Approach," *Journal of Engineering Mechanics*, Vol. 125, No. 11, 1999, pp. 1298–1307.

[15]Thomsen, O. T., "Modeling of Multi-Layer Sandwich Type Structures Using a High-Order Plate Formulation," *Journal of Sandwich Structures and Materials*, Vol. 2, No. 4, 2000, pp. 331–349.

[16]Thomsen, O. T., "High-Order Theory for the Analysis of Multi-Layer Plate Assemblies and its Application for the Analysis of Sandwich Panels with Terminating Plies," *Composite Structures*, Vol. 50, No. 3, 2000, pp. 227–238.

[17]Thomsen, O. T., and Frostig, Y., "Localized Bending Effects in Sandwich Panels: Photoelastic Investigation versus High-Order Sandwich Theory Results," *Composite Structures*, Vol. 37, No. 1, 1997, pp. 97–108.

[18]Swanson, S. R., "Response of Orthotropic Sandwich Plates to Concentrated Loading," *Journal of Sandwich Structures and Materials*, Vol. 2, No. 3, 2000, pp. 270–287.

[19]Stoer, J., and Bulirsch, R., *Introduction to Numerical Analysis*, Springer-Verlag, New York, 1993.

[20]Jensen, L. R., Rauhe, J. C., and Stegmann, J., "Finite Elements for Geometric Nonlinear Analysis of Composite Laminates and Sandwich Structures," M.S. Thesis, Inst. of Mechanical Engineering, Aalborg Univ., Aalborg, Denmark, 2001.

K. N. Shivakumar
Associate Editor